

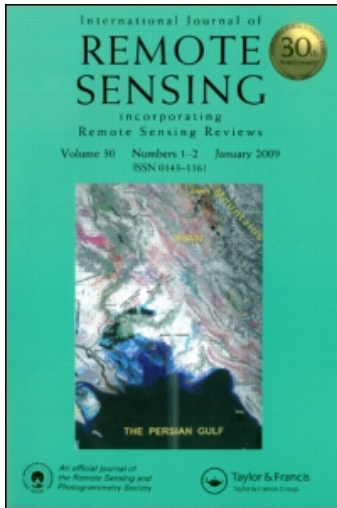
This article was downloaded by: [TIB / UB Hannover]

On: 7 October 2010

Access details: Access Details: [subscription number 915530145]

Publisher Taylor & Francis

Informa Ltd Registered in England and Wales Registered Number: 1072954 Registered office: Mortimer House, 37-41 Mortimer Street, London W1T 3JH, UK



International Journal of Remote Sensing

Publication details, including instructions for authors and subscription information:

<http://www.informaworld.com/smpp/title~content=t713722504>

Mapping Quaternary faults in the west of Kavir Plain, north-central Iran, from satellite imageries

A. Babaahmadi^a; A. Yassaghi^a; A. Naeimi^a; GH. R. Dini^b; S. Taghipour^c

^a Department of Geology, Tarbiat Modares University, Tehran, Iran ^b Leibniz University of Hannover, Institute for Photogrammetry and Geo-Information (IPI), Germany ^c School of Geology, The University of Tehran, Tehran, Iran

Online publication date: 06 October 2010

To cite this Article Babaahmadi, A. , Yassaghi, A. , Naeimi, A. , Dini, GH. R. and Taghipour, S.(2010) 'Mapping Quaternary faults in the west of Kavir Plain, north-central Iran, from satellite imageries', International Journal of Remote Sensing, 31: 19, 5111 – 5125

To link to this Article: DOI: 10.1080/01431160903283884

URL: <http://dx.doi.org/10.1080/01431160903283884>

PLEASE SCROLL DOWN FOR ARTICLE

Full terms and conditions of use: <http://www.informaworld.com/terms-and-conditions-of-access.pdf>

This article may be used for research, teaching and private study purposes. Any substantial or systematic reproduction, re-distribution, re-selling, loan or sub-licensing, systematic supply or distribution in any form to anyone is expressly forbidden.

The publisher does not give any warranty express or implied or make any representation that the contents will be complete or accurate or up to date. The accuracy of any instructions, formulae and drug doses should be independently verified with primary sources. The publisher shall not be liable for any loss, actions, claims, proceedings, demand or costs or damages whatsoever or howsoever caused arising directly or indirectly in connection with or arising out of the use of this material.

Mapping Quaternary faults in the west of Kavir Plain, north-central Iran, from satellite imageries

A. BABA AHMADI†, A. YASSAGHI*†, A. NAEIMI†, GH. R. DINI‡ and
S. TAGHIPOUR§

†Department of Geology, Tarbiat Modares University, PO Box 14115-175, Tehran, Iran

‡Leibniz University of Hannover, Institute for Photogrammetry
and Geo-Information (IPI), Germany

§School of Geology, The University of Tehran, Tehran, Iran

(Received 27 August 2008; in final form 17 January 2009)

Numerous Quaternary faults are found in north-central Iran with an insignificant history of seismic activity. Having either strike-slip or thrust mechanisms, these faults are potentially active and therefore capable of creating destructive earthquakes. In this paper, Landsat Enhanced Thematic Mapper Plus (ETM+) images were used, for the first time, to map these Quaternary faults located in an abandoned area to the west of Kavir Plain in north-central Iran. We also demonstrate the use of satellite imagery to identify Quaternary faults in an unpopulated area using geomorphological features, such as deformed quaternary alluviums, deflected stream channels, shutter ridges and sag ponds, and also fault scarps. The major mapped faults have two main northwest and northeast trends. These faults are following the trends of their counterparts in the eastern and western Alborz range. Despite the evidence of activity in the Quaternary faults, no large earthquakes have been recorded in the study area and therefore they can be considered as only potentially active faults. This is because of the lack of historically recorded earthquakes in the abandoned area in the past centuries or to extensively developed evaporate layers at depths that cause most of the recent deformations to occur aseismically.

1. Introduction

The central Iran structural zone forms a large triangular region within the Arabian–Eurasian continental collision zone (figure 1(a)). The presence of long active faults has been identified in northwest Zagros and in the southern part of Alborz bounding central Iran (e.g. Berberian 1976a, Bachmanov *et al.* 2004). In the east-southeast part of central Iran, active faults such as Doruneh, Nayband and Nehbandan faults with a long history of recorded earthquakes have also been described (e.g. Bonini *et al.* 2003, Walker and Jackson 2004). Despite several investigations being carried out on the identification of the active faults in the east-southeast part of central Iran (Berberian 1976a, Berberian and Yeats 1999, Berberian *et al.* 2001, Walker and Jackson 2002, 2004), the occurrence of destructive events is common, such as the 2003 Bam earthquake (magnitude (M_w) = 6.5), in which the earthquake surface rupture did not follow the known Bam faults (Fu *et al.* 2004, Talebian *et al.* 2004, Fu *et al.* 2007). This indicates that a large number of

*Corresponding author. Email: yassaghi@modares.ac.ir

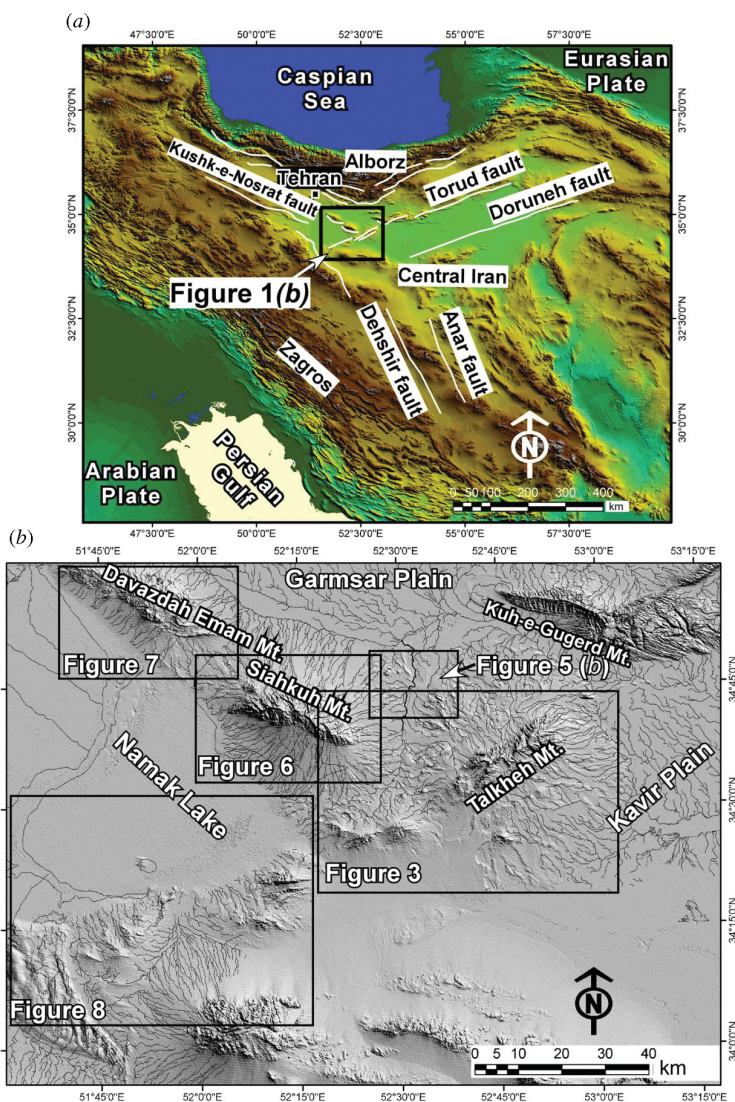


Figure 1. (a) The Arabian–Eurasian plate collision zone, showing the position of the study area located between the major faults in north-central Iran. (b) Details of the location of the later figures shown here on the Shuttle Radar Topography Mission (SRTM) image (90-m digital elevation model, DEM) of the study area.

unknown active faults exist, particularly in abandoned areas within central Iran. It is generally thought that the lack of evidence for the occurrence of large historical earthquakes in these regions should not be interpreted as a lack of seismic activity (e.g. Berberian 1976*b*). This is because of the long recurrence periods of earthquakes that exceed both historically and instrumentally recorded intervals.

Unlike the east-southeast part of central Iran, no detailed investigations have been performed on mapping of the active faults in the west of Kavir Plain in north-central Iran in which the study area is located. Despite the tectonic situation of this area, low seismic activity based on historically and instrumentally recorded earthquakes can be

inferred. Therefore, mapping of the Quaternary faults can provide the basis for identification of potentially active faults. The study area is located in an unapproachable and unpopulated area and almost all the fault kinematics indicators are obscured and would not be detected at fields because of their poor outcrops. Thus, remote sensing studies pave the way for mapping such Quaternary faults (e.g. Sabins 1997). In this paper, we report the use of Landsat Enhanced Thematic Mapper Plus (ETM+) imagery and aeromagnetic data, in attempts to map the Quaternary faults in the west of Kavir Plain in north-central Iran. This also demonstrates the capability of the interpretation of satellite imagery for identification of Quaternary faults in an abandoned area using geomorphological features.

2. Geological setting

The Cenozoic rocks comprise most of the outcrops in the west of Kavir Plain, while the older rocks crop out dispersed in anticline cores. Paleocene succession consists mainly of conglomerate and sandstone, mostly overlying older units as unconformity. Eocene rock formations in central Iran as well as the Lut block contain mostly thick-bedded lavas or volcanic rocks deposited in a marine basin (Berberian and King 1981). During the late Oligocene, this sea transgressed towards central Iran, leaving marine Oligocene–Miocene deposits. Thick terrestrial series of marl, limestone and red evaporates were also deposited in these basins. In the late Miocene, deposition of sandstone, marl, conglomerate and evaporate rocks developed in a molasses-type condition of sedimentary environment. The Pliocene succession, similar to that in other Iranian regions, consists of conglomerate, overlying older deposits as an unconformity. Quaternary deposits are classified as old alluvial fans known as Qt1 (Pleistocene) and young fans (Holocene) known as Qt2 (Emami 1991, Vahdati Daneshmand 1991). The study area is also covered by several sand dunes.

Three major depressions encircle the study area: Kavir Plain to the east, Qom-Aran to the west and Garmsar to the north (figure 1). These depressions are intercontinental basins filled with the detrital and evaporate deposits since the late Eocene (except for the Oligocene–Miocene interval). They were developed because of uplift of the surrounding area as a result of doming and/or subsidence of lowlands triggered by major strike-slip faults (see Berberian and King 1981).

3. Materials and methods

To map the Quaternary faults in this study, first the satellite data were radiometrically corrected. To recognize detailed objects for better performance in georectification, the related bands were then combined and radiometrically corrected. Orthorectification was also performed using 1:50 000 topography data and polynomial equations in the WGS84 as datum and the Universal Transverse Mercator (UTM) zone 39 as projection. For better recognition of geomorphological features, the 7-4-2 composite bands were made as well.

Furthermore, for reduction of data correlation and redundancy, principal component analysis (PCA) was performed. PCA is a technique that produces images among which the correlation is either zero or close to zero and reduces the number of bands without losing band information (Mather 2004). Therefore, PCA was performed in order to be replaced with a band that has the closest correlation with it. For band selection, scatter plots were obtained. They show that band 2 has the most correlation with the others. Therefore, PC1 was replaced with band 2 (0.53–0.61 μm) in order to recognize geological features, especially structural lineaments.

For better identification of rock units, faults and lineaments at a larger scale, multispectral ETM+ images with a 28.5-m cell size and the panchromatic band of the ETM+ image with a 14.25-m cell size were merged together by data fusion methods. Data fusion was performed by using the intensity–hue–saturation (IHS) method. In this method, a multispectral (ETM+) image is transformed from Red–Green–Blue (RGB) into IHS space, and then the intensity component of the image is replaced by the panchromatic band of the ETM+ image. Finally, inverse transformation from IHS space into RGB space was carried out. Contrast stretching, such as linear contrast stretching and histogram equalization, was also performed on the resulting image of data fusion.

The 7×7 edge sharpening filter has been used to detect more detail in the edges, which can be fault lineaments (see figure 2(a)):

$$7 \times 7 \text{ edge sharpening filter} \\ \begin{bmatrix} -1 & -1 & -1 & -1 & -1 \\ -1 & -1 & -1 & -1 & -1 \\ -1 & -1 & 49 & -1 & -1 \\ -1 & -1 & -1 & -1 & -1 \\ -1 & -1 & -1 & -1 & -1 \end{bmatrix}$$

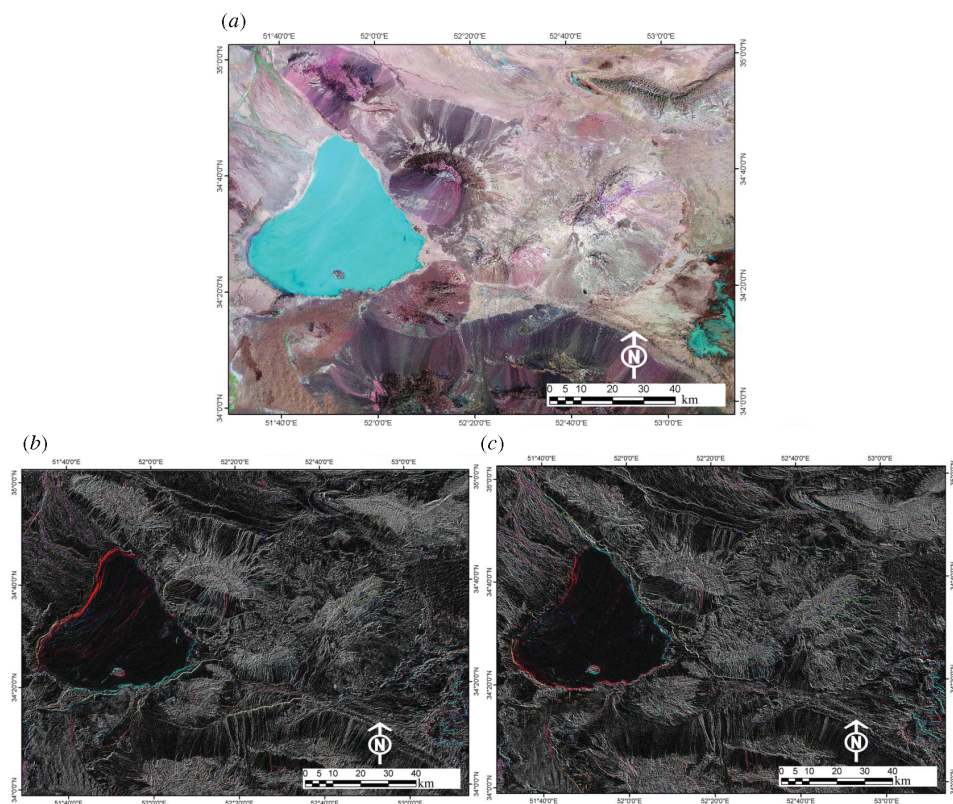


Figure 2. The ETM+ image of north-central Iran resulting from insertion (a) using the PCA technique, data fusion and 7×7 sharpening filters, (b) the NW Robinson three-level filter and (c) the NE Robinson three-level filter.

Among gradient filters, the Robinson three-level operator was also used in the northwest and northeast directions to detect similar trending fault lineaments. The Robinson three-level operator was then derived from the Prewitt operator. It is one of the derivative-based filters (Pratt (2001); figures 2(b) and 2(c)). The resulting images were used for mapping the Quaternary faults.

$$\begin{array}{cc}
 5 \times 5 \text{ NE Robinson three-level operator} & 5 \times 5 \text{ NW Robinson three-level operator} \\
 \begin{bmatrix} 0 & 0 & -1 & -1 & -1 \\ 0 & 0 & -1 & -1 & -1 \\ 1 & 1 & 0 & -1 & -1 \\ 1 & 1 & 1 & 0 & 0 \\ 1 & 1 & 1 & 0 & 0 \end{bmatrix} & \begin{bmatrix} -1 & -1 & -1 & 0 & 0 \\ -1 & -1 & -1 & 0 & 0 \\ -1 & -1 & 0 & 1 & 1 \\ 0 & 0 & 1 & 1 & 1 \\ 0 & 0 & 1 & 1 & 1 \end{bmatrix}
 \end{array}$$

4. Mapping Quaternary faults

Quaternary faults were mapped in the four major areas across north-central Iran: the Talkheh, Siahkuh, Davazdah Emam mountains and the southern part of Lake Namak (figure 1(b)).

4.1 Quaternary faults around Mt Talkheh

Mt Talkheh is an anticline with a core of Eocene volcanic rocks. The fold surface is composed of Oligo-Miocene as well as Miocene limestone and marl, which are highly sensitive to erosion and therefore exhibit smooth topography (figure 3). Pliocene conglomerates and Quaternary alluviums are observed in dark colours on the satellite images. Mt Talkheh is cut by northeast-trending Talkheh faults (TF1 and TF2 in figure 3).

The TF1 fault, which has deformed Quaternary alluviums on the northern slope of Mt Talkheh, is interpreted as a Quaternary fault. Evidence includes cross-cutting of a small fold developed in the Plio-Quaternary rock units and truncation of the alluvial fans to the north of Mt Talkheh (figure 4(c)). To the west of the TF1 fault, two other smaller faults have also been mapped. One of these faults has truncated an alluvial fan close to its apex, producing a fault scarp of several metres in height (figures 3(a) and 4(d)). The other one has cut across some alluvial fan bodies (figure 4(b)). To the south of the TF1 fault, Quaternary alluviums were displaced by about 500 m horizontally by one of the TF1 splays (figure 5(b)). To the north of Mt Talkheh there are a few sand dunes that have been cross-cut by a northeast-trending fault (figure 4(d)).

The southern flank of Mt Talkheh is also bisected by parallel TF3 and TF4 Quaternary faults (figure 3). These faults have cut and/or displaced laterally the Holocene alluviums and drainage channels as well as the rock units of Mt Talkheh and thus are interpreted as having a sinistral strike-slip mechanism (figure 3(a)). The TF3 and TF4 faults, in their northern part, have left-laterally offset a stream channel by approximately 1.5 and 2 km, respectively (figures 3(b) and 5(a)). It is generally thought that the lateral deflection of rivers and stream channels is indicative of active faults (Keller and Pinter 1996). The TF3 and TF4 fault scarps that have truncated the Quaternary alluviums are also clearly observed on the satellite image (figures 4(a) and 5(a)). A shutter ridge contributing to the deviation of the stream channels is also seen along the TF3 (figures 3(b) and 4(a)). In addition, development of sag ponds along the strike of the TF3 fault constrains its dominant strike-slip mechanism (figure 3(b)).

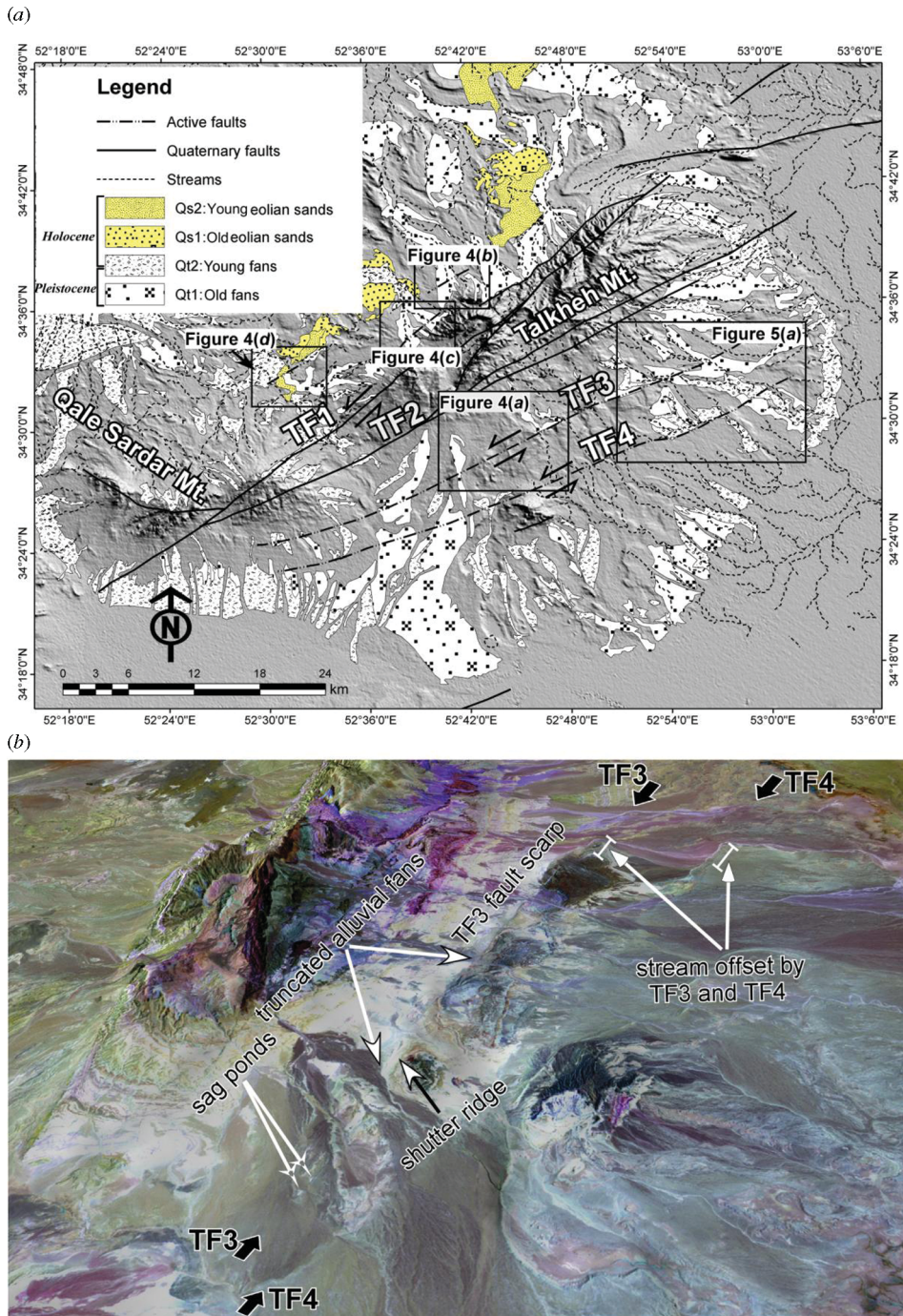


Figure 3. (a) Map of Quaternary faults around Mt Talkheh on the Shuttle Radar Topography Mission (SRTM) image (90-m digital elevation model, DEM). (b) Structural and geomorphological interpretation of the TF3 and TF4 faults on the 3D view of the ETM+ image superimposed on the SRTM DEM (vertical exaggeration: 5×).

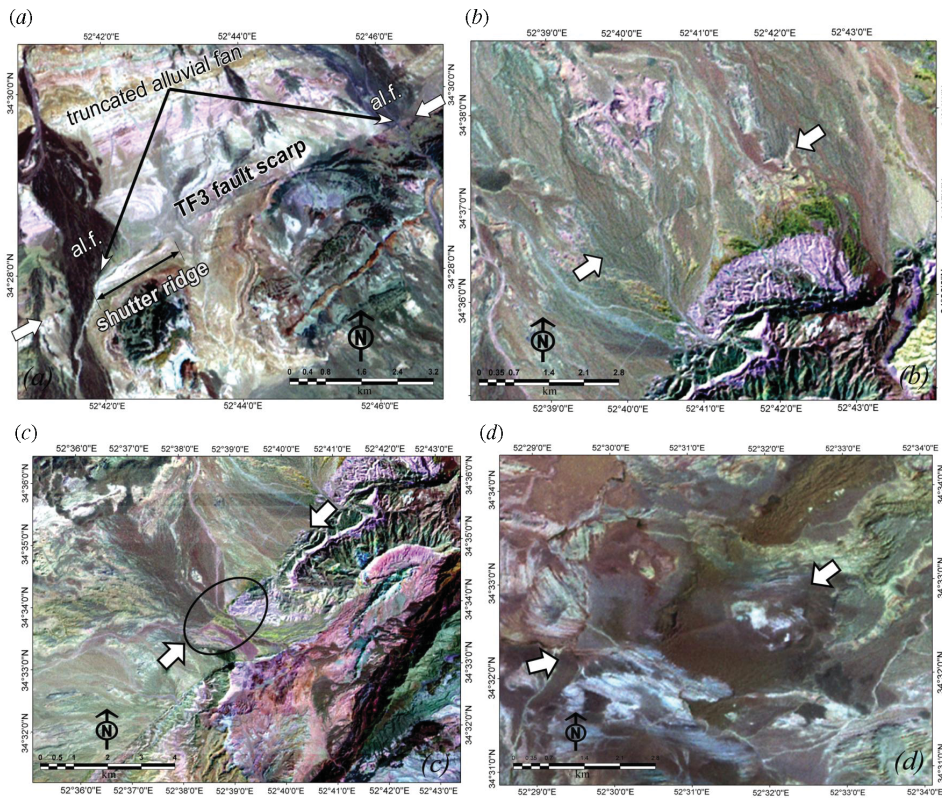


Figure 4. (a) An image of the TF3 fault scarp that cut alluvial fans (al.f.). Note the development of a shutter ridge along the fault. (b) Truncation of a small fault to the west by the TF1 in the north of Mt Talkheh. (c) Truncation of alluvial fans by the TF1 in the north of Mt Talkheh. (d) Truncation of sand dunes and Quaternary alluviums by a small quaternary fault in the north of Mt Talkheh. Refer to figure 3(a) for the location of these images within the study area.

To the west of Mt Talkheh there is a river, Talkhab River, that flows from south to north (figures 1(b) and 5(b)). This river has been deflected right-laterally by the northwest-trending TF5 fault (figure 5(b)). In addition, to the west of the Talkhab River, there is a dry river channel that is thought to be an abandoned channel of the Talkhab River because of reactivation of the TF5 fault. The effect of the TF5 fault can also be seen on the Quaternary deposits in the vicinity of the Talkhab River (figure 5(b)).

4.2 Quaternary faults around Mt Siahkuh

Like Mt Talkheh, the Siahkuh mountain is an anticline in which the Eocene volcanic rocks constitute the fold core and the Oligo-Miocene limestone and marl crop out in the fold limbs (figures 1(b) and 6). The fold southern limb has been cut by the northeastern-dipping Siahkuh thrust fault along which Mt Siahkuh thrust over the Quaternary deposits (figures 6(a) and 6(b)). Channel incisions have occurred on rivers crossing the Siahkuh thrust, causing the younger alluvial fans to form downslopes away from their former locus (figure 6(b)). As argued by Keller and Pinter (1996), such an incision is due to the continuous uplift of the Siahkuh thrust and hence indicates its recent

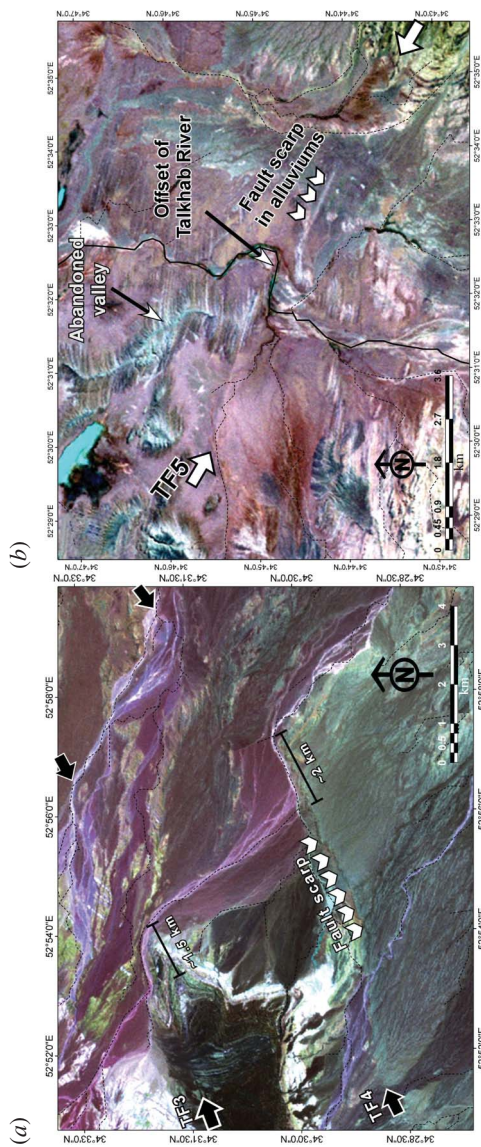


Figure 5. (a) Streams offset by TF3 and TF4. Scale bars (1.5 and 2 km) are given for the offset amount. Note the development of a fault scarp along the TF3. Refer to figure 3(a) for the location of this image within the study area. (b) The Talkhab River offset by the TF5 fault. An abandoned channel is observed in the north of the fault zone. Refer to figure 1(b) for the location of this image within the study area.

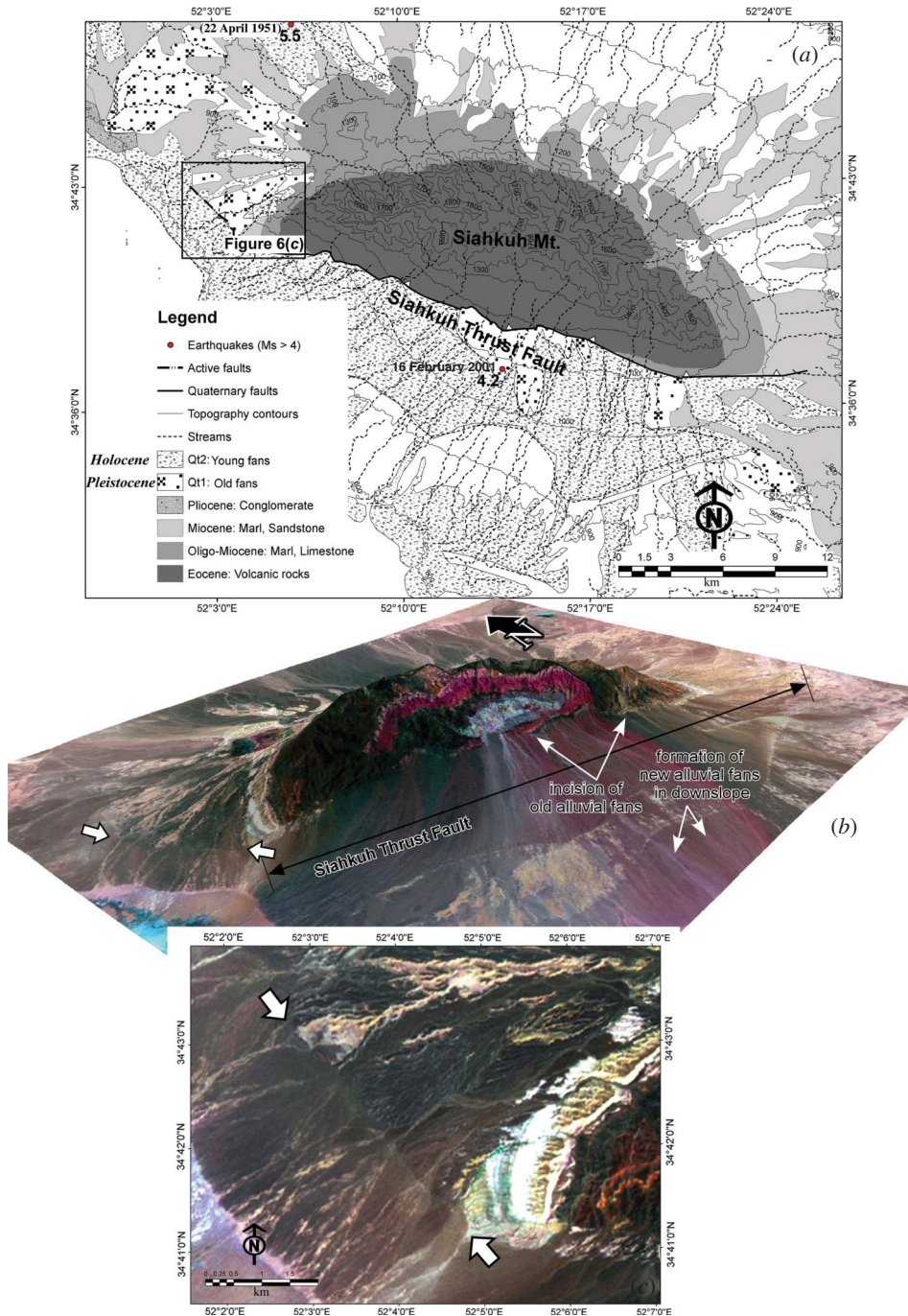


Figure 6. (a) Map of the Siahkuh fault region. (b) The 3D view of the ETM+ image superimposed on the Shuttle Radar Topography Mission (SRM) 90-m digital elevation model (DEM) (vertical exaggeration: 5×) of the Siahkuh fault. (c) The active segment of the Siahkuh thrust in which old alluvial fans thrust over the young alluvial fans. Refer to figure 1(b) for the location of these images within the study area.

activity. Along the western part of the fault, the older alluvial fans with a darker colour and rougher morphology thrust over the younger ones (figure 6(c)).

4.3 Quaternary faults around Mt Davazdah Emam

Mt Davazdah Emam, located to the north of Lake Namak, is composed of Eocene volcanic rocks, Oligocene–Miocene and Miocene limestone and marl units, and Pliocene conglomerate (figures 1(b) and 7(a)). The Davazdah Emam fault thrust the Eocene volcanic rocks over a series of younger rock units from the Oligocene–Miocene to recent alluvium deposits (figure 7(b)). This thrust fault is composed of a set of parallel faults, one of which has cut alluvial fans close to the apex in the south of Mt Davazdah Emam, suggesting the Quaternary nature of the fault (figure 7(c)). To the south of the Davazdah Emam fault, Pliocene and Miocene rock units are folded to form a large anticline in which its northern limb has been cut by the fault (figure 7(b)). On the satellite image of this anticline, the Pliocene conglomerate has a darker colour and rougher topography than the Miocene rock units (figure 7(b)). Like the Siahkuh fault, along the Davazdah Emam fault channel incisions have occurred in the older alluvial fans resulting in deposition of younger alluvial fans downwards away from their former places (figure 7(b)). This geomorphological evidence as well as the epicentre of the 1937 [magnitude (M_w) = 5.4] and 2007 (M_w = 4.6) earthquakes along the Davazdah Emam fault indicates that this is an active fault.

4.4 Quaternary faults to the south of Lake Namak

To the south of Lake Namak, three faults with different trends have been mapped that have cut Quaternary deposits and sand dunes (figures 1(b) and 8(a)). These faults have been named Maranjab-1, Maranjab-2 and Maranjab-3. The northeast-trending Maranjab-1 fault that has a 50-km-long linear trace on satellite images of cut Quaternary alluviums, alluvial fans, stream channels and sand dunes and is therefore considered as a Quaternary fault (figure 8(b)). The Maranjab-1 fault, forming the southern boundary of the Namak Lake, is a high angle fault interpreted as controlling development of the Namak Lake basin (figure 8).

The northeast-trending Maranjab-2 fault that is located to the south of the Maranjab-1 fault forms the structural boundary between sand dunes and Quaternary deposits and in places crossing the sand dunes as well (figure 8(b)). Detailed mapping of the fault on the satellite images reveals that the Maranjab-2 fault can be divided into three segments. The Maranjab-2 fault terminates at the northwest-trending Maranjab-3 fault, which crosses the northern limb of a Plio-Quaternary syncline (figure 8(b)). The southern limb of the syncline has also been vertically incised by an east-trending stream. It is thought that such a rapid uplift of the syncline is most probably due to Quaternary activity of the Maranjab-3 fault.

5. Discussion

The active tectonics in the Iranian plateau is thought to be related to the continental collision between the Arabian and Eurasian plates (Vita-Finzi 2001). With regard to the present-day deformation on major active faults in the Iranian plateau, shortening occurred approximately 3–7 million years ago (Allen *et al.* 2004). Since that time, the continental collision continues in the general north-northeast trending across the suture zone between the Arabian and Eurasian plates and at a rate of 22 mm year⁻¹ based on

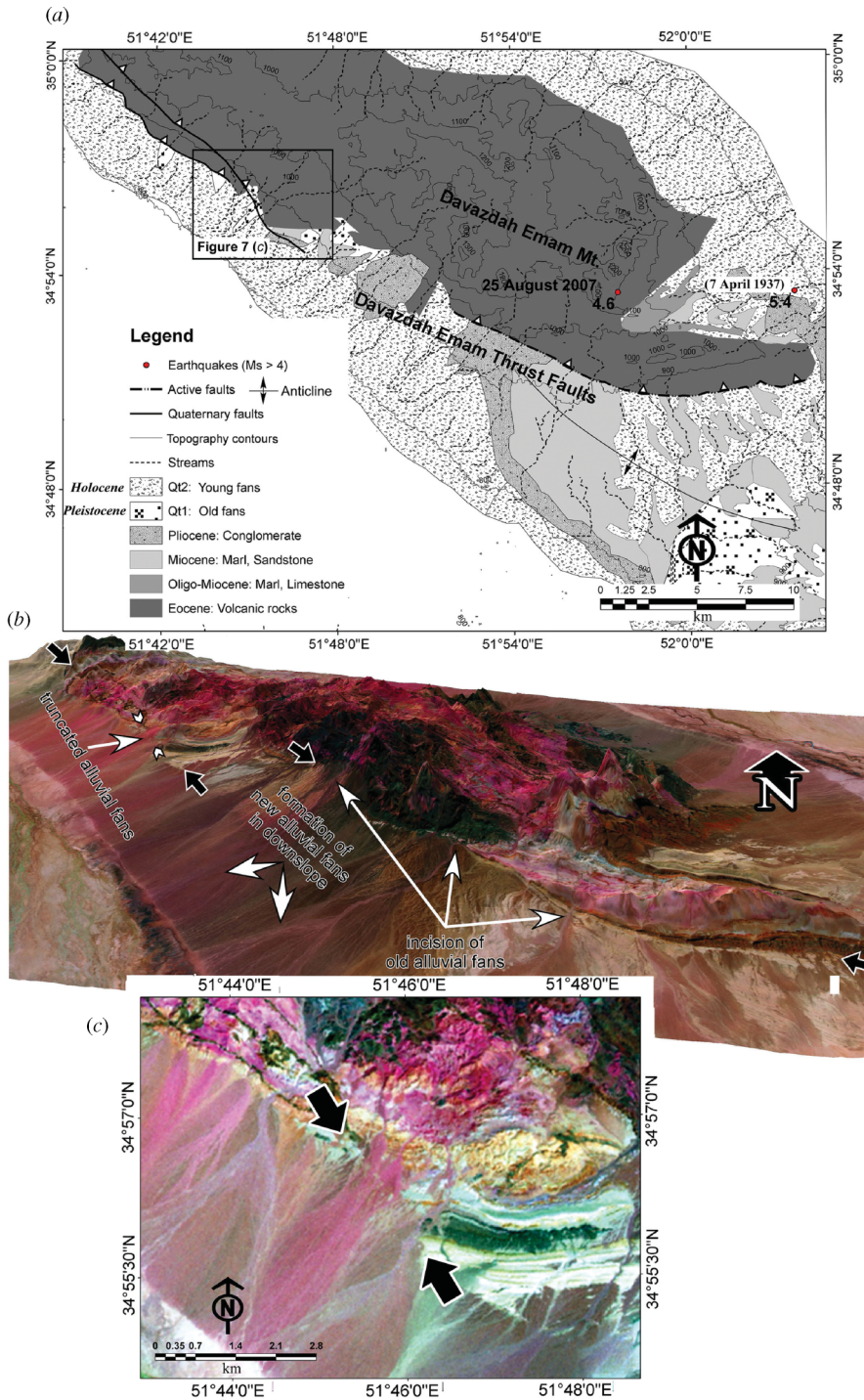


Figure 7. (a) Map of Mt Davazdah Emam. (b) The 3D view of the ETM+ image superimposed on the Shuttle Radar Topography Mission (SRTM) 90-m digital elevation model (DEM) (vertical exaggeration: $5\times$) of the Davazdah Emam thrust. (c) Truncation of Quaternary alluviums by the Davazdah Emam fault. Refer to figure 1(b) for the location of these images within the study area.

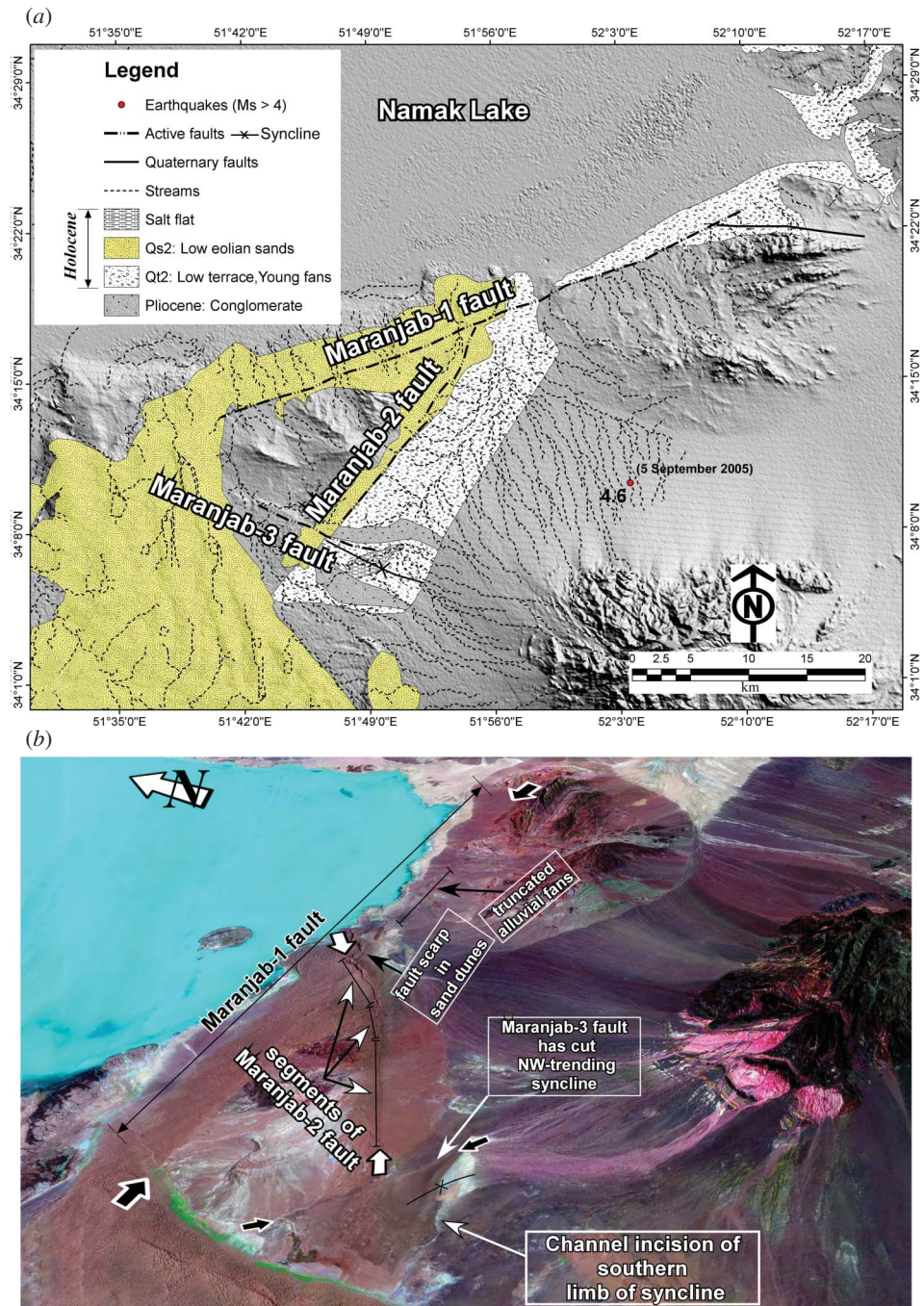


Figure 8. (a) Map of the southern part of Lake Namak and (b) the 3D view of the ETM+ image superimposed on the Shuttle Radar Topography Mission (SRTM) 90-m digital elevation model (DEM) (vertical exaggeration: $7\times$) of the active faults (Maranjab-1, Maranjab-2 and Maranjab-3).

Global Positioning System (GPS) measurements. In central Iran, however, the shortening occurs in a north–south direction and at a rate of about 2 mm year^{-1} (Vernant *et al.* 2004b). This shortening rate was also measured as 3 mm year^{-1} by Vernant *et al.* (2004a) across the Pishva thrust, which is a Quaternary fault located in north-central Iran. The north–south shortening in central Iran is apparently caused by anticlockwise rotation of crustal blocks, bounded by the right-lateral Dehshir and Anar strike-slip faults (figure 1(a)), about vertical axes (Walker and Jackson 2004). This crustal block rotation is interpreted as resulting in reactivation of the Quaternary faults in the study area.

The Siahkuh, Davazdah Emam, Talkheh and Maranjab faults are major Quaternary structural elements in the study area. The faults trends vary from northeast trending (the Talkheh and Maranjab faults) to northwest trending (the Siahkuh and Davazdah Emam faults) (figure 1(b)). These trends follow their counterpart in the Alborz range in which active deformation within the broad region of the Arabian–Eurasian continental collision occurs (Allen *et al.* 2003). These two main groups of fault trends have also been detected on the magnetic basement lineaments map of Iran (Yousefi and Friedberg (1994); figure 9(a)). According to this map, most of the mapped faults in the study area are deep-seated basement structures that have been reactivated since the Late Pliocene (Berberian *et al.* 2001). It is proposed that the Talkheh and Maranjab-1 faults are in fact the southern continuation of the left-lateral northeast-trending Torud active fault (figure 1(a)). The 1953 earthquake ($M_w = 6.5$) is interpreted as occurring due to reactivation of the Torud fault (Berberian 1976b). Furthermore, the Siahkuh and Davazdah Emam faults are inferred to be a continuation of the northwest-trending Kushk-e-Nosrat and Avaj active faults (figure 1(a)) (see Hessami *et al.* (2003)).

Although central Iran has experienced shallow earthquakes with surface faulting, large magnitudes and several hundred years of recurrence intervals (e.g. the 1968 Dasht-e-Bayaz earthquake with $M_w = 7.4$ and the 1978 Tabas earthquake with $M_w = 7.6$) (Berberian and Yeats 1999, Masson *et al.* 2005, Engdahl *et al.* 2006), the study area located in north-central Iran exhibits low seismic activity and no large earthquakes have been detected instrumentally (figure 9(b)). Lack of knowledge on

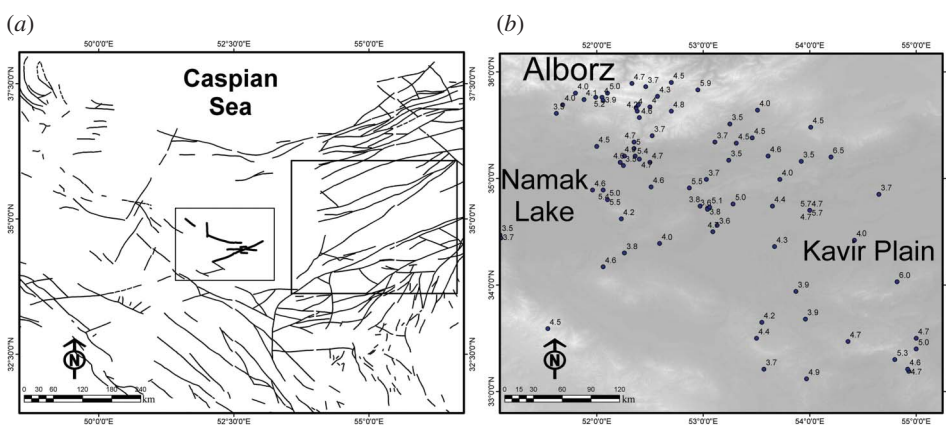


Figure 9. (a) Basement lineaments of north-central Iran drawn from the aeromagnetic map of Iran at scale 1:2 500 000 (Yousefi and Friedberg 1994). The small rectangle shows the western part of the Kavir Plain (the study area) and the large rectangle shows the central part of the Kavir Plain. (b) Distribution of the instrumental earthquake epicentres in the small rectangle area (after: <http://www.iiees.ac.ir> from 1922 to 2008). Numbers are earthquake magnitudes.

historical earthquakes in such areas should not be considered as due to a lack of large earthquakes (Berberian 1976b). This is because the recurrence periods of large earthquakes exceed intervals historically as well as records instrumentally. The very low shortening rate of 3 mm year^{-1} in north-central Iran, as suggested by Vernant *et al.* (2004a), constrains this interpretation.

6. Conclusions

The morphotectonics evidence presented in this study for mapping Quaternary faults in north-central Iran comprises cut recent deposits, offset and deflected streams and also linear features such as shutter ridges and sag ponds along faults. Application of these geomorphological features to the identification of Quaternary faults in an abandoned area has also verified the capability of the interpretation of satellite imagery. Although these features cannot prove the active nature of the faults, due to lack of historical as well as instrumental seismicity along them, they could indicate that the mapped Quaternary faults are potentially active. This is because their earthquake recurrence intervals are probably longer than the history of such abandoned areas. The low seismic activity of the study area might also be due to the presence of ductile evaporates at depths that led the faults to have aseismic activity. The circular to spheroidal shape of some of these folds as well as the existence of salt diapirs to the south of Garmsar Plain, especially around Mt Kuh-e-Gugerd, represent the broad deposition of such evaporates in north-central Iran.

Acknowledgements

We thank Dr M. Sartaj for providing the raw data and H. Mehregan and E. Tavakkolian for their helpful collaboration.

References

- ALLEN, M.B., GHASEMI, M.R., SHAHRABI, M. and QORASHI, M., 2003, Accommodation of late Cenozoic oblique shortening in the Alborz range, northern Iran. *Journal of Structural Geology*, **25**, pp. 659–672.
- ALLEN, M.B., JACKSON, J. and WALKER, R.T., 2004, Late Cenozoic reorganization of the Arabia–Eurasia collision and the comparison of short-term and long-term deformation rates. *Tectonics*, **23**, pp. 1–16.
- BACHMANOV, D.M., TRIFONOV, V.G., HESSAMI, K., KOZHURIN, A.I., IVANOV, T.P., ROGOZHIN, E.A., HADEMI, M.C. and JAMALI, F.H., 2004, Active faults in the Zagros and central Iran. *Tectonophysics*, **380**, pp. 221–241.
- BERBERIAN, M., 1976a, Documented earthquake faults in Iran. In *Geological Survey of Iran*. Report No. 39, pp. 173–183 (Tehran: Geological Survey of Iran).
- BERBERIAN, M., 1976b, Contribution to the seismotectonics of Iran. In *Geological Survey of Iran*. Report No. 39, pp. 76–96 (Tehran: Geological Survey of Iran).
- BERBERIAN, M., JACKSON, J.A., FIELDING, E., PARSONS, B., PRIESTLEY, K., QORASHI, M., TALEBIAN, M., WALKER, R., WRIGHT, T.J. and BAKER, C., 2001, The 1998 March 14 Fandoqa earthquake (M_w 6.6) in Kerman province, southeast Iran: re-rupture of the 1981 Sirch earthquake fault, triggering of slip on adjacent thrusts and the active tectonics of the Gowk fault zone. *Geophysical Journal International*, **146**, pp. 371–398.
- BERBERIAN, M. and KING, G.C.P., 1981, Towards a palaeogeography and tectonic evolution of Iran. *Canadian Journal of Earth Science*, **18**, pp. 210–265.
- BERBERIAN, M. and YEATS, R.S., 1999, Patterns of historical earthquakes rupture in the Iranian plateau. *Bulletin of the Seismological Society of America*, **89**, pp. 120–139.

- BONINI, M., CORTI, G., SOKOUTIS, D., VANNUCCI, G., GASPERINI, P. and CLOETINGH, S., 2003, Insights from scaled analogue modeling into the seismotectonics of the Iranian region. *Tectonophysics*, **376**, pp.137–149.
- EMAMI, M.H., 1991, *Geological Map of Aran, Scale 1:250000* (Tehran: Geological Survey of Iran).
- ENGDahl, E.R., JACKSON, J., MYERS, S.C., BERGMAN, E.A. and PRIESTLEY, K., 2006, Relocation and assessment of seismicity in the Iran region. *Geophysical Journal International*, **167**, pp. 761–778.
- FU, B.H., LEI, X.L., HESSAMI, K., NINOMIYA, Y., AZAMA, T. and KONDO, K., 2007, A new fault rupture scenario for the 2003 M_w 6.6 Bam earthquake, SE Iran: insights from the high-resolution QuickBird imagery and field observations. *Journal of Geodynamics*, **44**, pp. 160–172.
- FU, B.H., NINOMIYA, Y., LEI, X.L., TODA, S. and AWATA, Y., 2004, Mapping the active strike-slip fault triggered the 2003 M_w 6.6 Bam, Iran, earthquake with ASTER 3D images. *Remote Sensing of Environment*, **92**, pp. 153–157.
- HESSAMI, K., JAMALI, F. and TABASSI, H., 2003, *Major Active Faults of Iran, Scale 1:2500000* (Tehran: International Institute of Earthquakes Engineering and Seismology).
- KELLER, E.A. and PINTER, N., 1996, *Active Tectonics, Earthquakes, Uplift and Landscape* (Englewood Cliffs, NJ: Prentice Hall).
- MASSON, F., CHERY, J., HATZFELD, D., MARTINOD, J., VERNANT, P., TAVAKOLI, F. and GHAFORY-ASHTIANI, M., 2005, Seismic versus aseismic deformation in Iran inferred from earthquake and geodetic data. *Geophysical Journal International*, **160**, pp. 217–226.
- MATHER, P.M., 2004, *Computer Processing of Remotely-Sensed Images* (New York: John Wiley & Sons, Inc.).
- PRATT, W.K., 2001, *Digital Image Processing*, 3rd edition, p. 735 (New York: John Wiley & Sons, Inc.).
- SABINS, F., 1997, *Remote Sensing: Principles and Interpretation* (New York: W.H. Freeman and Company).
- TALEBIAN, M., FIELDING, E.J., FUNNING, G.J., JACKSON, J., NAZARI, H., PARSONS, B., PRIESTLY, K., QORASHI, M., ROSEN, P.A., WALKER, R. and WRIGHT, T.J., 2004, The 2003 Bam (Iran) earthquake: rupture of a blind strike-slip fault. *Geophysical Research Letters*, **31**, L11611, doi:10.1029/2004GL020058.
- VAHDATI DANESHMAND, F., 1991, *Geological Map of Kuh-e-Gugerd, Scale 1:250000* (Tehran: Geological Survey of Iran).
- VERNANT, P., NILFOROUSHAN, F., CHERY, J., BAYER, R., DJAMOUR, Y., MASSON, F., NANKALI, H., RITZ, J.F., SEDIGHI, M. and TAVAKOLI, F., 2004a, Deciphering oblique shortening of central Alborz in Iran using geodetic data. *Earth and Planetary Science Letters*, **223**, pp. 177–185.
- VERNANT, P., NILFOROUSHAN, F., HATZFELD, D., ABBASSI, M.R., VIGNY, C., MASSON, F., NANKALI, H., MARTINOD, J., ASHTIANI, A., BAYER, R., TAVAKOLI, F. and CHERY, J., 2004b, Present-day crustal deformation and plate kinematics in the Middle East constrained by GPS measurements in Iran and Northern Oman. *Geophysical Journal International*, **157**, pp. 381–398.
- VITA-FINZI, C., 2001, Neotectonics at the Arabian plate margins. *Journal of Structural Geology*, **23**, pp. 521–530.
- WALKER, R.T. and JACKSON, J., 2002, Offset and evolution of the Gowk fault, S.E. Iran: a major intra-continental strike-slip system. *Journal of Structural Geology*, **24**, pp. 1677–1698.
- WALKER, R.T. and JACKSON, J., 2004, Active tectonics and late Cenozoic strain distribution in central and eastern Iran. *Tectonics*, **23**, TC5010, doi:10.1029/2003TC001529.
- YOUSEFI, H. and FRIEDBERG, N., 1994, *Aeromagnetic Map of Iran, Scale 1:2500000* (Tehran: Geological Survey of Iran).